DIAMOND-LIKE CARBON (DLC) AS ADHESION PROMOTING INTERLAYER IN STEEL / EPOXY-BASED CFRP HYBRID LAMINATES

A. Monden[1*], M.G.R. Sause[1]

[1]University of Augsburg, Augsburg, Germany

ABSTRACT: Four different diamond-like carbon (DLC) coating variants were investigated via different experimental techniques to assess their suitability as adhesion promoting interlayers in intrinsic steel/epoxy-based CFRP hybrid laminates. Sandwich specimens with a symmetrical layup consisting of unidirectional CFRP with a thin, surface modified steel layer in the center plane were investigated. The DLC variants were compared to other types of commonly used surface modifications via SBS (short-beam shear) tests. Subsequently, the two most promising DLC variants (high hardness, DLC-HH and Silicon-doped, DLC:Si) were further investigated. Commonly used testing procedures like DCB (double cantilever beam), ENF (3-point end-notched flexure) and MMB (mixed-mode beam) tests were adapted to assess the fracture toughness at the interface. SBS tests after hot/wet ageing showed a trend from brittle to ductile failure behaviour for DLC-HH and for DLC:Si vice versa. Thus, XPS (X-ray photoelectron spectroscopy) measurements were conducted to detect changes of the surface chemical composition and functional groups caused by hot/wet ageing. Finally, potentiostatic and potentiodynamic measurements proved the corrosion resistance of the DLC variants. The conducted investigations proved a high potential of DLC-coatings as interlayers for metal/epoxy-based CFRP structures.

KEYWORDS: CFRP/steel hybrid laminate, surface modification, diamond-like carbon (DLC), fracture toughness, interfacial failure, corrosion resistance

1 INTRODUCTION

Reliable use of hybrid structures and materials depends on the availability of mechanically and chemically stable joint technologies for combining fiber reinforced plastics (FRP) and metals [1-4]. While combinations of lightweight metals and FRP are used in aerospace applications, steel is still the most widely used construction material in other fields of engineering, often due to economic reasons. Integration of structural FRP parts in such industrial areas leads inevitably to the challenge of joining these different material classes. Due to their different chemical structure, direct joints of steel and epoxy resin will result in poor adhesion, which leads to the requirement of surface treatments and modifications to achieve a mechanically and chemically stable joint. In case of CFRP, direct contact between carbon-fibers and the surface of the metallic constituent may lead to galvanic corrosion [5, 6]. Using an additional layer of a polymer (e.g. adhesive or resin) or GFRP to insulate the carbon-fibers from the metal surface will usually deteriorate the mechanical properties. Thus, surface modifications applied to the metallic constituent, which are capable of inhibiting galvanic corrosion, are preferred. Diamond-like carbon (DLC) coatings in general are amorphous, metastable carbon-based materials exhibiting a significant ratio of sp^3-hybridized C-bonds, which account for the diamond-like properties like high hardness, chemical stability and low electrical conductivity [7, 8]. Therefore, DLC coatings are considered as promising candidate for an interlayer in intrinsic CFRP/metal hybrid laminates. Within this study, four different DLC coating variants were investigated regarding their suitability to fulfill the above-mentioned requirements.

2 SCREENING VIA SHORT-BEAM SHEAR TESTS

Within a screening, four different DLC variants were applied to X5CrNi18-10 cold-rolled steel foils of 0.1 mm nominal thickness using a PACVD (plasma-assisted chemical vapour deposition) process. With the choice of

* Corresponding author: Andreas Monden, Mechanical Engineering, Institute of Materials Resource Management, University of Augsburg, Universitätsstr. 1, D-86135 Augsburg, Germany, Phone +49-[0]821-598-3453, Fax +49-[0]821-598-3411, andreas.monden@mrm.uni-augsburg.de

reactive gas (hydrocarbon precursor), the hydrogen content (C/H-ratio) of the coating can be influenced [7, 8]. DLC coatings may be doped with e.g. Silicon to reduce residual stresses of the coating and thus improve adhesion to the steel substrate [8, 9]. Doping may be achieved by using a Silicon containing hydrocarbon precursor. Further, Si-doping may change the surface chemistry regarding steel/DLC and DLC/epoxy adhesion. We investigated two "standard" DLC variants, one with relatively high hardness (DLC-HH) and one with lower hardness (DLC-LH), a multilayer-variant (DLC-ML) consisting of a DLC-HH base layer and a DLC-LH top layer, and a silicon-doped variant (DLC:Si). Typical coating thicknesses are 2 - 3 µm for a monolayer and 5 - 7 µm for the multilayer variant, respectively.
Subsequently, sandwich plates were fabricated using a symmetrical layup consisting of 10 layers of SGL CE 1250-230-39 unidirectional epoxy-based prepreg with a nominal thickness of 0.22 mm per layer in cured state and the DLC coated steel foils laminated at the center plane. A standard curing cycle using 130 °C temperature for 90 min following the materials supplier's recommendations was used. Besides the DLC variants, a variety of commonly used surface modifications was applied to the steel foils prior to co-curing them with the prepreg material to enable a direct comparison [10, 11]. After laminating and curing the sandwich plates, samples of 20 mm length, 10 mm width and 2.4 mm resulting thickness were cut from the cured laminates using a dry diamond saw cutting process to avoid preliminary delamination at the CFRP-metal interface due to moisture expansion or in-take. The surface modifications were compared to an untreated reference (hybrid laminate with cleaned and degreased, "as-received" steel surface) and monolithic CFRP via short-beam shear (SBS) tests [10, 11] following DIN EN 2563. Results of the SBS tests and optical microscopy images of the resultant delamination surfaces are shown in Fig. 1.

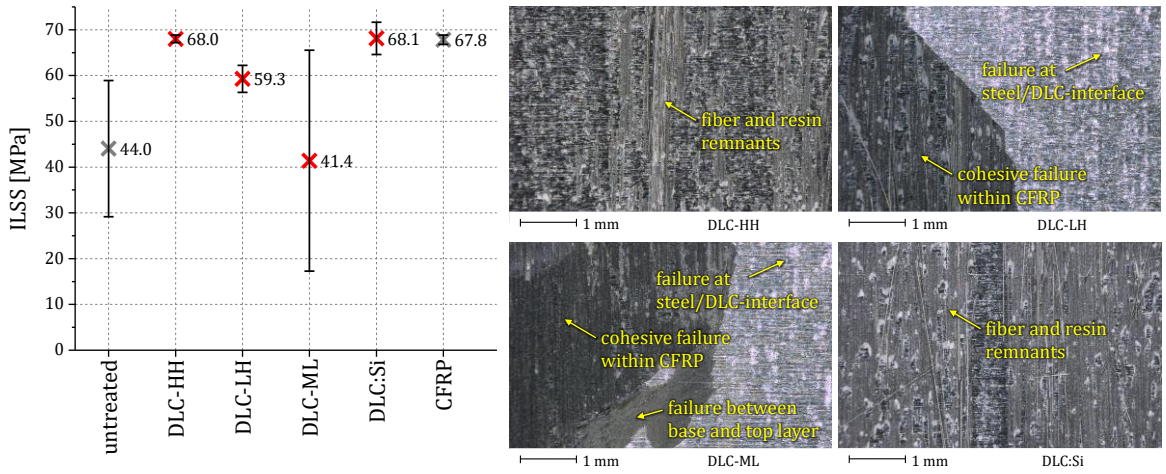

Fig. 1 *Apparent interlaminar shear-strength (ILSS) values obtained via SBS tests on three samples each and representative optical microscopy images of the resultant delamination surfaces* [11]

The DLC-LH and DLC-ML variants showed partial failure at the steel/DLC interface, with additional failure between base and top layer for the DLC-ML. DLC-HH and DLC:Si showed mainly cohesive failure within CFRP and at the same time reached ILSS values comparable to the monolithic CFRP. Therefore, those two variants were investigated more closely.

3 FRACTURE MECHANICAL CHARACTERIZATION

The fracture toughness at the interface of symmetrical hybrid laminates with DLC-HH and DLC:Si coatings was determined under mode I, mode II and mixed-mode load conditions. In this case, the laminates consisted of 14 layers of the epoxy-based CFRP prepreg and the DLC coated steel foils laminated at the center plane, resulting in a thickness of 3.4 mm. At one side of the steel foil, a precrack was built in using ETFE-foil of 25 µm thickness (Wrightlon® 5200).
DCB tests were conducted in accordance with ASTM D5528. Specimens of 200 mm length, 20 mm width and 50 mm effective precrack length were cut from the cured plates. Force during testing was applied via adhesively bonded load blocks and a crosshead speed of 5 mm/min. Crack tip propagation was recorded using a digital camera system (Zwick VideoXtens) enabling post-evaluation of initiation and propagation values.
In case of ENF tests in accordance with ASTM D7905, specimens of 175 mm length, 20 mm width and 48 mm precrack length (30 mm effective precrack length during fracture testing) were used. Tests were conducted with a crosshead speed of 0.8 mm/min. Delamination initiation was recorded and post-evaluated via digital image correlation (DIC) techniques (GOM ARAMIS 12M) [12].

MMB tests were conducted in accordance with ASTM D6671, and three different mode mixities (Eq. 1) were applied by variation of the lever arm length of the MMB testing apparatus.

$$0 < \frac{G_{\mathrm{II}}}{G} = \frac{G_{\mathrm{II}}}{G_{\mathrm{I}} + G_{\mathrm{II}}} < 1 \qquad (1)$$

Specimens of 150 mm length, 20 mm width and 28 mm effective precrack length were used. Tests were conducted with a crosshead speed of 0.5 mm/min. As for the ENF tests, delamination initiation was recorded and post-evaluated via DIC techniques.
Corrections of the measured (apparent) fracture toughness values are necessary to account for a variety of effects. In case of DCB tests, corrections for large displacements and the stiffening of the specimen by the end blocks are performed according to ASTM D5528. For MMB tests, lever arm weight has to be taken into account, which results in a shift of the intended mode mixities towards higher mode II ratios in the present case. The investigated hybrid laminates exhibit a macroscopically symmetrical layup, whereas failure is initiated at one of the CFRP/steel interfaces and thus asymmetry is introduced in the vicinity of the crack tip. For DCB tests, this asymmetry results in a minor mode II contribution, which can be estimated by the semi-empirical relationship established by MOLLÓN et. al. [13]. In case of MMB tests, similar effects on mode mixity result from the asymmetric failure behavior, which can be estimated using the formalism introduced by SHAHVERDI et. al. [14]. Thermally induced residual stresses resulting from curing at elevated temperatures affect the apparent fracture toughness values and the resultant mode mixities. This influence was quantified using the formulas proposed by YOKOZEKI et. al. [15], which are based on the general relationship introduced by NAIRN [16].
Results shown in Fig. 2 are based on six specimens in case of DCB tests and three specimens in case of MMB and ENF tests, respectively. In case of untreated steel surfaces, purely adhesive failure at the interface was observed for the entirety of investigated mode mixities.

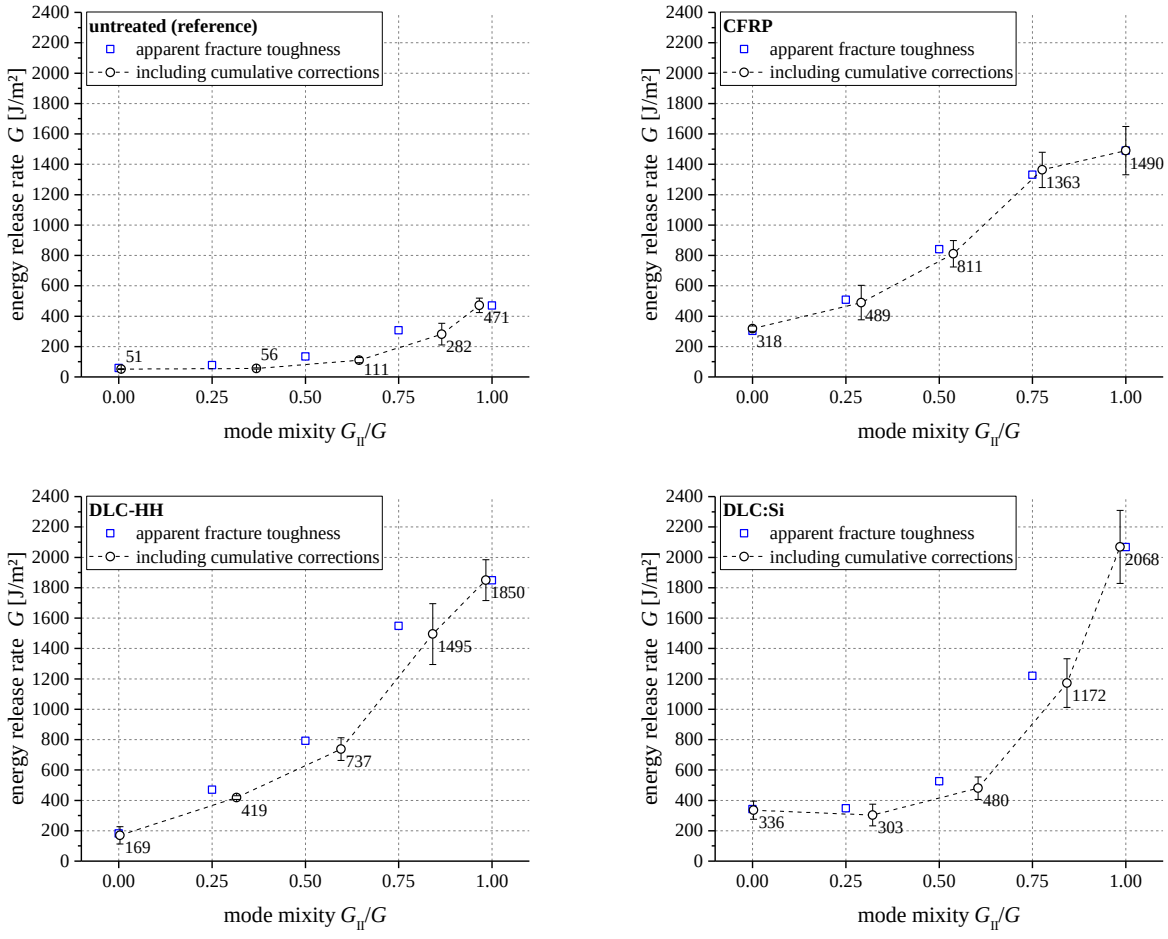

Fig. 2 *Fracture mechanics results including apparent fracture toughness values (as measured) and cumulative corrections* [11, 17].

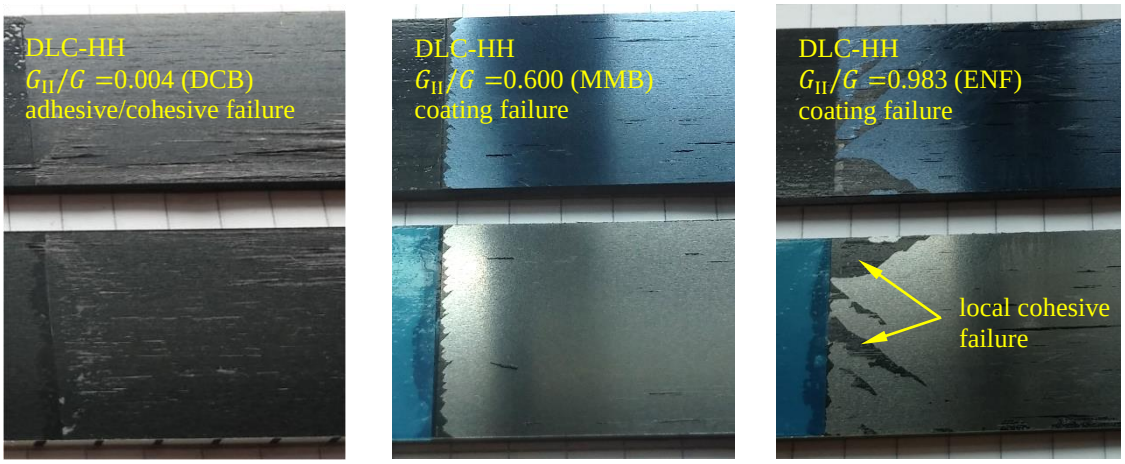

Fig. 3 *Fracture surfaces of DLC-HH coated specimens (representative examples)* [11, 17]*. Upper row: CFRP side, lower row: Steel side.*

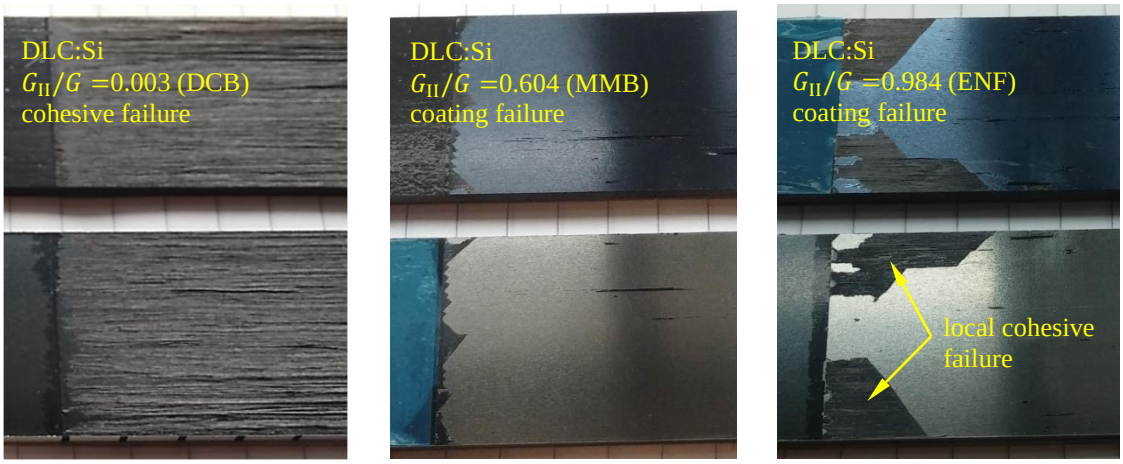

Fig. 4 *Fracture surfaces of DLC:Si coated specimens (representative examples)* [11, 17]*. Upper row: CFRP side, lower row: Steel side.*

Mode I fracture toughness was significantly increased by DLC:Si coatings and exceeded the fracture toughness of pure CFRP. Observation of crack surfaces coincides with these findings, exhibiting purely cohesive failure within CFRP (Fig. 4). In the mixed-mode regime, coating failure was observed for both DLC coatings. Fracture toughness values of monolithic CFRP were nearly reached by DLC-HH. Both investigated DLC coatings exceeded the mode II fracture toughness of pure CFRP significantly, but exhibited coating failure at the steel/DLC interface (Fig. 3, 4). Further investigations carried out on combinations of Al_2O_3 grit blasting and DLC coatings indicate a further potential of fracture toughness increase mainly in the mode I-dominated regime due to mechanical interlocking [11, 17]. Overall, the investigated DLC coatings proved suitable to improve fracture toughness across the whole range of investigated mode mixities.

4 HOT/WET AGEING AND X-RAY PHOTOELECTRON SPECTROSCOPY

To investigate the influence of hot/wet environment on the bonding strength, SBS tests were conducted on specimens after ageing at 85 °C / 85 %RH for 3 and 12 days, respectively. Exemplary shear stress vs. displacement curves are shown in Fig. 5. Interestingly, the failure behaviour changed from brittle to ductile in case of DLC-HH and for DLC:Si vice versa.
To investigate the changes caused by hot/wet ageing, XPS (X-ray photoelectron spectroscopy) measurements on DLC coated steel samples of both variants were conducted before and after ageing at 85 °C / 85 %RH for 14 days.

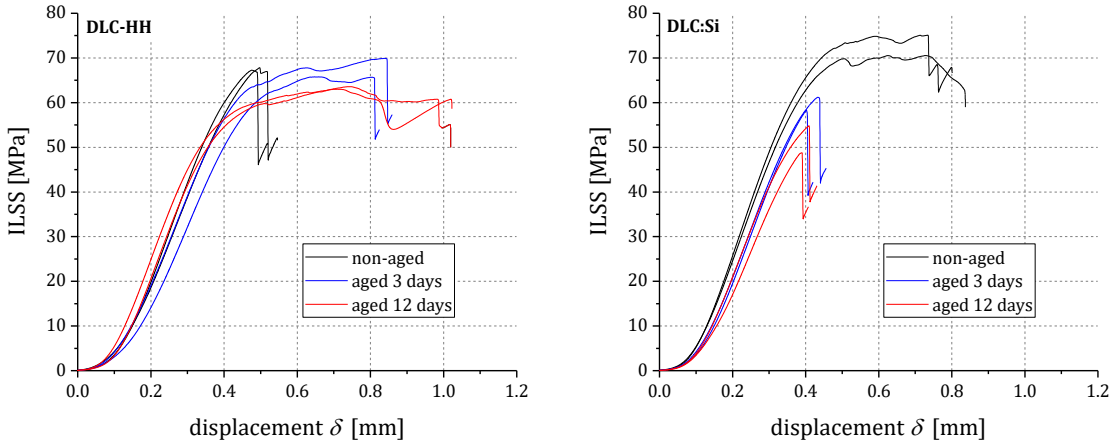

Fig. 5 *Exemplary shear stress vs. displacement curves showing contrary effect of hot/wet ageing* [11].

In case of DLC-HH, no significant changes of elementary composition were observed (Table 1), with Oxygen indicating an existence of functional groups. Investigation of the C1s-peak did not show significant changes concerning the existence of functional chemical groups (Table 2). C–C and C–H bonds represent the largest share of chemical bonds determined, which is typical for the DLC type investigated within this study (a-C:H, amorphous Carbon with significant Hydrogen content [7, 8]). The good adhesive properties of DLC towards epoxy resins may be attributed to the existence of functional chemical groups like C–OR, C=O and COOR [18]. As the XPS technique resembles a particularly surface-sensitive spectroscopic technique (information depth ≤ 3 nm [19]), changes at the interface between steel substrate and DLC layer or within the volume of the DLC layer are not accessible. It has already been shown within this paper that the adhesion between steel substrate and DLC coating contributes to the global failure behaviour of the investigated hybrid laminates. Thus, chemical changes at the steel/DLC-interface or within the DLC layer due to hot/wet ageing may alter the failure behaviour.

Table 1: *Elemental composition of DLC-HH before and after hot/wet ageing* [11].

	C [at%]	O [at%]	N [at%]
DLC-HH non-aged	87.2	10.8	1.5
DLC-HH aged 14 days	87.8	11.8	0.5

Table 2: *Chemical bonds and functional groups determined by investigation of the C1s-peak of DLC-HH before and after hot/wet ageing* [11].

	C–C [%]	C–H [%]	C–OR [%]	C=O [%]	COOR [%]	Shake-up [%]
DLC-HH non-aged	52.0	34.6	7.2	3.7	1.9	0.5
DLC-HH aged 14 days	52.0	34.1	7.8	3.4	2.0	0.6

In case of DLC:Si, the Silicon-content is clearly detectable and exhibits a stoichiometric composition of $C_{2.65x}Si_x$ in non-aged state and $C_{1.67x}Si_x$ after hot/wet ageing, respectively (Table 3). At the same time, the Oxygen content clearly increases. From Table 4 it can be seen that the share of Si–C- and C–H-bonds at the surface is significantly reduced while the share of C–C-bonds is increased. The share of functional groups (e.g. C–OR, C=O, COOR) does not change significantly. Table 5 shows the oxidation of the present Silicon: The share of $Si(–O)_2$ and $Si(–O)_3$ increases at the expense of Si–C and $Si(–O)_1$. In summary, this indicates a simultaneous breaking up of Si–C-bonds and formation of SiO_x-precipitations at or near the DLC-surface, being the governing mechanism altering the global failure behaviour of the laminate towards behaving more brittle. At the same time, the formation of SiO_x-precipitations may lead to a concentration gradient inducing diffusion of Silicon towards the surface. In this scenario, the steel/DLC-interface may be depleted from Silicon, deteriorating the adhesive properties at the steel/DLC-interface and thus contributing to the alteration of the global failure behaviour and deteriorating the mechanical properties of the whole laminate.

Table 3: *Elemental composition of DLC:Si before and after hot/wet ageing* [11].

	C [at%]	O [at%]	N [at%]	Si [at%]
DLC:Si non-aged	58.3	15.7	4.0	22.0
DLC:Si aged 14 days	45.5	24.5	2.8	27.2

Table 4: *Chemical bonds and functional groups determined by investigation of the C1s-peak of DLC:Si before and after hot/wet ageing* [11].

	Si–C [%]	C–C [%]	C–H [%]	C–OR [%]	C=O [%]	COOR [%]	Shake-up [%]
DLC:Si non-aged	19.1	37.6	32.4	6.3	2.1	2.6	-
DLC:Si aged 14 days	11.7	53.9	21.7	8.1	2.1	2.5	-

Table 5: *Chemical bonds and functional groups determined by investigation of the Si2p-peak of DLC:Si before and after hot/wet ageing* [11].

	Si–C [%]	$Si(–O)_1$ [%]	$Si(–O)_2$ [%]	$Si(–O)_3$ [%]	$Si(–O)_4$ [%]
DLC:Si non-aged	40.9	41.9	5.4	11.9	-
DLC:Si aged 14 days	22.2	36.5	10.0	31.3	-

5 CORROSION MEASUREMENTS

Besides the adhesion promoting properties of DLC-coatings, their corrosion inhibiting properties are relevant for practical applications. Thus, potentiodynamic and potentiostatic corrosion measurements were conducted on a measurement setup like shown in Fig. 6.

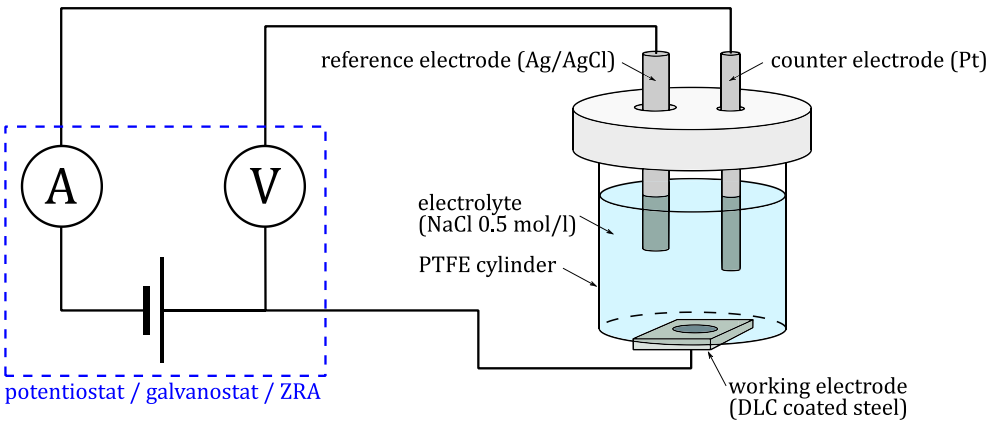

Fig. 6 *Schematic of measurement setup used for electrochemical experiments* [11, 20].

The measurement setup shown represents a three-electrode system with the sample used as working electrode. Potentials applied to the sample always have the Ag/AgCl-reference electrode as reference point and electric currents flow solely between sample and Pt-counter electrode. A potentiostat (type Interface 1000, Gamry Instruments) is used to measure or apply electrical currents and voltages, respectively, and can be utilized as potentiostat, galvanostat or zero resistance ammeter (ZRA). Hence, both stable DC voltages can be generated to conduct potentiodynamic polarization scans (PPS), as well as high-precision current measurements of galvanic corrosion processes can be conducted.

For PPS, the sample is polarized either cathodic or anodic via an external, variable voltage. The corresponding currents give information about the extent of the prevailing cathodic or anodic reaction. When plotting the voltage against the logarithmic current (EVANS diagram), characteristic regions may be distinguished. In this study, DLC-HH and DLC:Si coated steel was compared towards CFRP and uncoated steel (X5CrNi18-10) as a reference. From the EVANS diagram shown in Fig. 7 (left) it can be seen that the current is significantly reduced both in the cathodic ($E < E_{corr}$) as well as in the anodic ($E > E_{corr}$) region for both DLC coatings in

comparison to the uncoated steel surface. Both DLC coatings show an atypical trend in contrast to the uncoated steel surface, as passivation does not occur. Instead, the current I just moderately increases with increasing potential difference E even at regions $E \geq 0.5$ V, where pitting corrosion sets in for the uncoated steel surface. No significant increase of electrical current is observable even up to high potential differences, which indicates that pitting was completely inhibited.

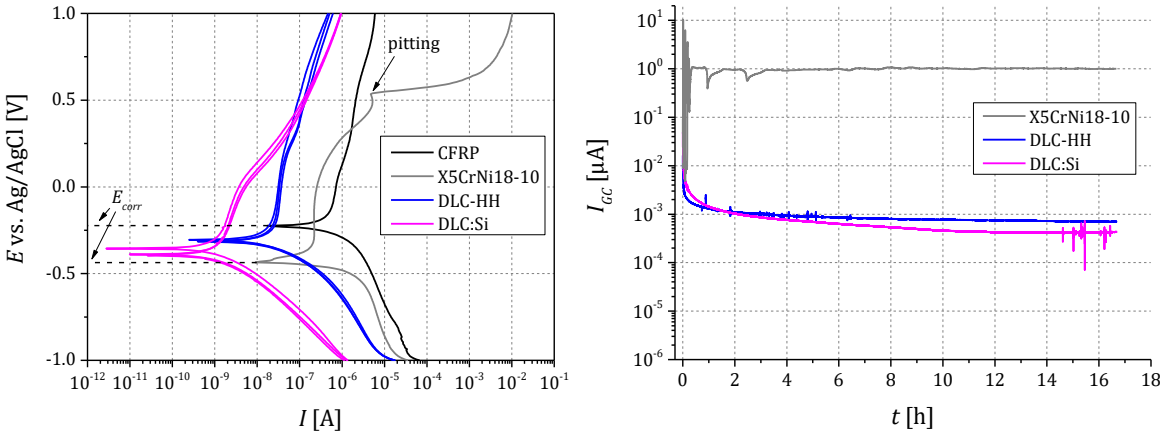

Fig. 7 *EVANS diagrams of potentiodynamic polarization scans of three DLC-HH and DLC:Si samples each (left); Galvanic corrosion against CFRP via potentiostatic measurements (right)* [11, 20].

Potentiostatic measurements showed, that the galvanic corrosion current I_{GC} against CFRP was reduced by a minimum of three orders of magnitude compared to an uncoated steel surface by both variants (Fig. 7, right).

6 CONCLUSIONS

Four DLC variants were compared against a variety of commonly used surface modification techniques via SBS tests. Among these, the two most promising variants (DLC-HH and DLC:Si) were investigated more detailed via different experimental techniques.

Compared to untreated specimen, DLC coatings showed a significant improvement of interfacial fracture toughness, which could be confirmed by examination of the fracture surfaces, revealing cohesive failure within the CFRP laminate or coating failure, respectively, depending on the applied load condition. Both variants exceeded the Mode II values of monolithic CFRP significantly, whereas the Mode I values of monolithic CFRP were exceeded by DLC:Si. In the mixed-mode regime, values of monolithic CFRP were nearly reached by DLC-HH. Corrections were needed to account for asymmetric failure behaviour and residual thermal stresses, affecting the mode mixities and measured (apparent) fracture toughness values.

SBS tests after hot/wet ageing showed a trend from brittle to ductile failure behaviour for DLC-HH and for DLC:Si vice versa. XPS measurements indicated a formation of SiO_x-precipitations at the DLC:Si surface and thus a depletion of the steel/DLC:Si interface from Si accounting for a weakening of this interface.

Potentiostatic and potentiodynamic measurements proved the corrosion resistance of the DLC variants: Pitting corrosion could be inhibited up to high potential differences and corrosion current densities could be reduced by three magnitudes compared to an uncoated steel surface.

The conducted investigations proved a high potential of DLC-coatings as interlayers for metal/epoxy-based CFRP structures. Their application towards hybrid structures based on thermoplastic matrices is currently under investigation.

7 ACKNOWLEDGEMENT

This work was conducted within the project “FORCiM³A – Forschungsverbund CFK/Metall-Mischbauweisen im Maschinen- und Anlagenbau“, which was funded by the Bayerische Forschungsstiftung (BFS). The authors take this opportunity to gratefully acknowledge the collaboration with Alexander Hartwig (Anwenderzentrum Material- und Umweltforschung, University of Augsburg), Claus Hammerl (AxynTec Dünnschichttechnik GmbH) and Marcus Kuhn (KUHN Beschichtungen GmbH).

REFERENCES

[1] Baldan A.: *Review: Adhesively-bonded joints and repairs in metallic alloys, polymers and composite materials: Adhesives, adhesion theories and surface pretreatment.* Journal of Materials Science, 39:1–49, 2004.
[2] Baldan A.: *Review: Adhesively-bonded joints in metallic alloys, polymers and composite materials: Mechanical and environmental durability performance.* Journal of Materials Science, 39:4729–4797, 2004.
[3] Venables J.D.: *Review: Adhesion and durability of metal-polymer bonds.* Journal of Materials Science, 19:2431–2453, 1984.
[4] Sinmazçelik T., Avcu E., Bora M.Ö., Çoban O.: *A review: Fibre metal laminates, background, bonding types and applied test methods.* Materials and Design, 32:3671–3685, 2011.
[5] Tavakkolizadeh M., Saadatmanesh H.: *Galvanic corrosion of carbon and steel in aggressive environments.* Journal Of Composites For Construction, 5(3):200–210, 2001.
[6] Peng Z., Nie X.: *Galvanic corrosion property of contacts between carbon fiber cloth materials and typical metal alloys in an aggressive environment.* Surface and Coatings Technology, 215(0):85–89, 2013.
[7] Robertson J.: *Diamond-like amorphous carbon.* Materials Science and Engineering R, 37:129–281, 2002.
[8] Grill A.: *Diamond-like carbon: state of the art.* Diamond and Related Materials, 8:428–434, 1999.
[9] Damasceno J.C., Camargo Jr S.S., Freire Jr F.L., Carius R.: *Deposition of Si-DLC films with high hardness, low stress and high deposition rates.* Surface and Coatings Technology, 133-134:247–252, 2000.
[10] Monden A., Sause M.G.R., Hartwig A., Hammerl C., Karl H., Horn S.: *Evaluation of Surface modified CFRP-Metal Hybrid Laminates.* In: Proceedings of Euro Hybrid Materials and Structures 2014, 2014.
[11] Monden A.: *Adhäsion zwischen epoxidharzbasiertem CFK und oberflächenmodifiziertem Stahl: Grenzschichtversagen von Hybridlaminaten unter Mode I, Mode II und Mixed-Mode Belastung.* PhD thesis, University of Augsburg, 2016.
[12] Sause M.G.R.: *In Situ Monitoring of Fiber Reinforced Composites.* Springer International Publishing, 2016.
[13] Mollón V., Bonhomme J., Vina J., Argüelles A.: *Theoretical and experimental analysis of carbon epoxy asymmetric dcb specimens to characterize mixed mode fracture toughness.* Polymer Testing, 29:766–770, 2010.
[14] Shahverdi M., Vassilopoulos A.P., Keller T.: *Mixed-Mode I/II fracture behavior of asymmetric adhesively-bonded pultruded composite joints.* Engineering Fracture Mechanics, 115:43–59, 2014.
[15] Yokozeki T., Ogasawara T., Aoki T.: *Correction method for evaluation of interfacial fracture toughness of DCB, ENF and MMB specimens with residual thermal stresses.* Composites Science and Technology, 68:760–767, 2008.
[16] Nairn J.A.: *On the calculation of energy release rates for cracked laminates with residual stresses.* International Journal of Fracture, 139:267–293, 2006.
[17] Monden A., Sause M.G.R., Horn S.: *Surface modified Steel/Epoxy-based CFRP Hybrid Laminates under Mode I, Mode II and Mixed-Mode Load Conditions.* In: Proceedings of 17th European Conference on Composite Materials, 2016.
[18] Moosburger-Will J., Jäger J., Strauch J., Bauer M., Lachner E., Horn S.: *Fiber matrix adhesion in carbon fiber reinforced epoxy resin: influence of surface chemistry and surface morphology.* (to be submitted).
[19] Seah M. P.: *A review of the analysis of surfaces and thin films by AES and XPS*. Vacuum, 34:3-4, 463–478 (1984).
[20] Hartwig A.: *Titandioxid als Korrosionsschutz von X5CrNi18-10 Edelstahl und dessen Einsatzmöglichkeit in CFK-Metall Hybridstrukturen*. PhD thesis, University of Augsburg, 2015.